

# The effect of aging and slurry density on triaxial shear properties of liquefied stabilized soil mixed with fiber material cured at the indoor and in-situ

Hung Khac Le<sup>(1)</sup>, Yukihiro Kohata<sup>(2)</sup>

## Abstract

In this study, a series of Consolidated–Undrained triaxial compression tests were conducted at a constant axial strain rate, with a small unloading and reloading during the monotonic loading to investigate the effect of various densities and curing times on the mechanical properties of Liquefied Stabilized Soil (LSS). The comparison of LSS mixed with fiber material in the amounts of 0 and 10 kg/cm<sup>3</sup> cured at the indoor and in-situ was discussed. Based on the test results, the effect of slurry density on the strength of LSS was found to be greater than the effect of curing time. The pre-peak behavior of  $q \sim \epsilon_a$  curve became more non-linear under the effect of changing slurry density, in contrast to the effect of curing time. Moreover, the damage degree of LSS with shearing becomes smaller with curing time, while it seems to be rather independent of slurry density.

**Keywords:** liquefied stabilized soil, fiber material, cured at indoor and in-situ, triaxial shear property

## 1. Introduction

Nowadays, environmental issues are arising from growing urbanization, especially in developing countries. Urban construction generates large amounts of construction waste soil that may not be appropriate for reuse in construction and may be harmful to the environment if not properly treated. Moreover, due to its small land area, the city confronts environmental issues such as a lack of ultimate waste disposal sites and resource limitations, such as concerns about the potential exhaustion of mineral resources, and the waste and recycling problem has become a societal issue. The problem has received considerable attention. Therefore, it is desirable to use recycled-oriented materials. The Liquefied Stabilized Soil (LSS)<sup>1)</sup> is one of cement-stabilized soil, improves the soil properties by the effect of cementation arising in an excavated soil mixed with cement and water, and has been extensively used in Japan. However, there is concern that the increased use of cement solidifiers in LSS increases their strength and causes them to behave brittlely, reducing their seismic resistance. In order to improve brittle property, Kohata et al 2), 3), proposed using pulverized newspaper as a fibered material to reinforce LSS, and conducted a series of unconfined and triaxial compression tests. The study found that after the peak of the stress-strain curve, LSS mixed with fibered material had improved brittle properties. Afterward, numerous investigations into the strength and deformation properties of LSS with fiber were conducted<sup>2), 3)</sup>. Nevertheless, no comprehensive investigation of LSS with fiber under a variety of combination conditions has been performed. Especially, the effect of various slurry densities and longer curing times on the strength and deformation properties of LSS cured at in-situ conditions is not clearly. In this study, a series of undrained triaxial compression tests were performed to investigate the effects of slurry density and curing time on the triaxial shear properties of LSS under various conditions. Base on the test results, the comparison between the strength and deformation properties of LSS cured at indoor and in-situ were discussed.

## 2. Test procedure

### 2.1. Test material

In this study, the New Snow Fine Clay (NSF-Clay), which is a commercially cohesive soil, was used as the homogenous base material. The physical property of NFS- clay are shown in Table 1. The cement stabilizer (Geoset 200 by Taiheiyo Cement Co., Ltd.) was used as the solidification agent. For the fiber material, newspaper, which is easy to obtain, was pulverized with water by a food processor and made into a cotton-like material.

**Table 1 : Physical parameters of NSF-CLAY**

Particle density $\rho_s$ (g/cm <sup>3</sup> )	2.762
Liquid limit $w_L$ (%)	60.15
Plastic limit $w_P$ (%)	35.69
Plasticity Index $I_P$	24.46

### 2.2. Mixing and specimen preparation

There are two types of mixing methods for LSS, that is, the “slurry method” and the “adjusted slurry method”. In this study, LSS were

(1) Graduate School of Engineering, Muroran Institute of Technology, Muroran Japan

(2) Professor, Muroran Institute of Technology, Muroran, Japan

Date of receipt: 15/4/2022

Editing date: 6/5/2022

Post approval date: 5/9/2022

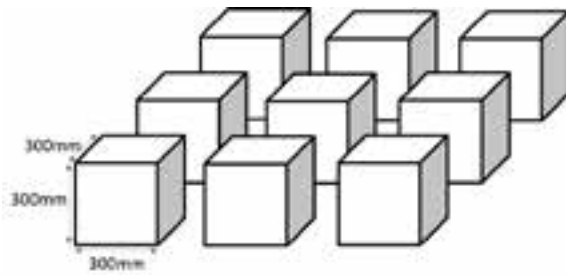


Figure 1: Schematic diagram of pits

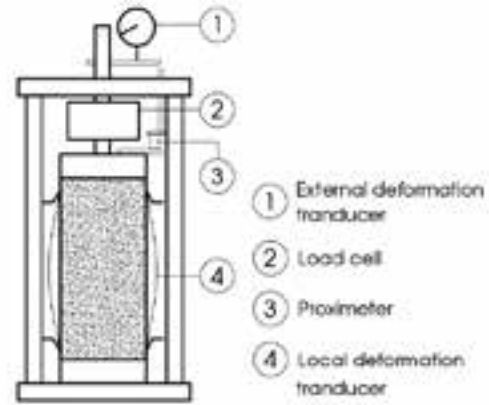


Figure 2: Schematic diagram of test apparatus

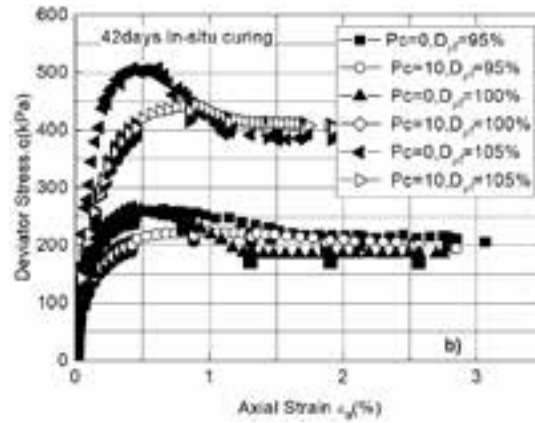
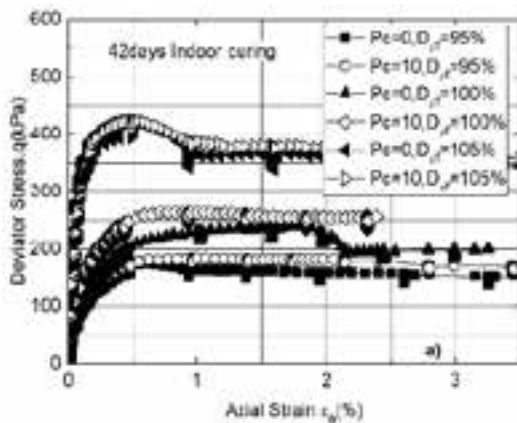


Figure 3: q vs  $\epsilon_a$  relation at 42 days indoor curing

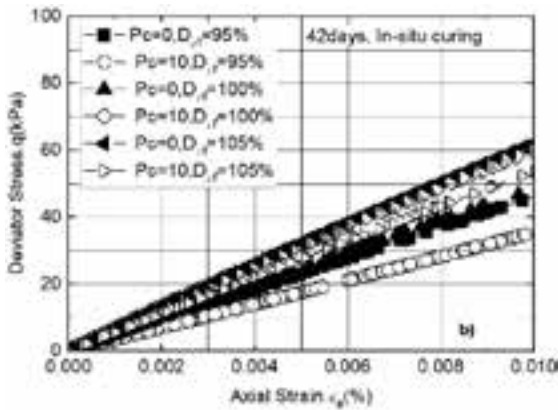
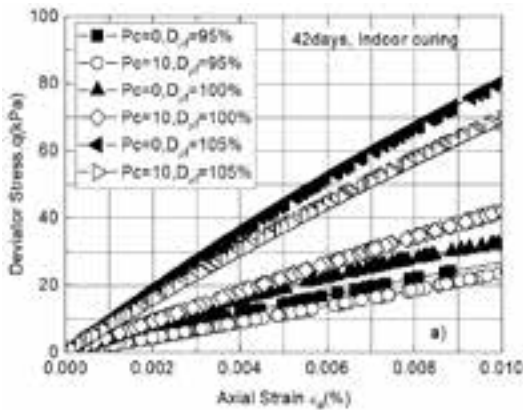


Figure 4: q vs  $\epsilon_a$  relation at 42 days in-situ curing

prepared by the “slurry method” because it is easier for preparation, in which NSF-Clay is mixed with an appropriate amount of water to produce a density-controlled slurry, which is then mixed with cement stabilizer and fiber material.

In order to investigate the effect of various slurry density on the strength and deformation of LSS reinforced fiber material, the basic slurry density was decided to be 1.280g/cm<sup>3</sup>, the density was base on the standard mix proportion design figure<sup>2</sup>), and the slurry density changing rate  $D_{pf}$  (actual slurry density)/ (basic slurry density) x 100% was defined as,  $D_{pf}=100\%$  ( $\rho_f=1.280\text{g/cm}^3$ ),  $D_{pf}=105\%$  ( $\rho_f=1.344\text{g/cm}^3$ ),  $D_{pf}=95\%$  ( $\rho_f=1.216\text{g/cm}^3$ ), respectively. To achieve the desired slurry density, this slurry was poured into a stainless steel container (AE mortar container) of 400cm<sup>3</sup> in volume and the excess portion was slipped off with a glass plate to

measure its density. After adjusting the slurry several times to obtain the required density, cement stabilizer in the amount of 100 kg/m<sup>3</sup> was added to the slurry. The amount of fiber material added was referenced as being 10 kg/m<sup>3</sup> based on a previous study<sup>2,3</sup>) (1.963g/specimen). After adding the fiber material, the Liquefied Stabilized Soil (LSS) was mixed with a hand-type mixer. Before filling the mold, the indoor-cured specimens were deaired by a negative pressure of about -90kPa for 30 minutes and put in a 50×100mm commercial plastic mold with fabric tape on top for extra filler. After filling the container with treated soil, a plastic film was attached to the top edge. The excess portion of fill was trimmed off after 3 hours of curing. The top surface was flattened, re-covered with polymer film, covered with a wet towel, and cured in moist air at 20±3°C. For the in-situ cured specimens, they

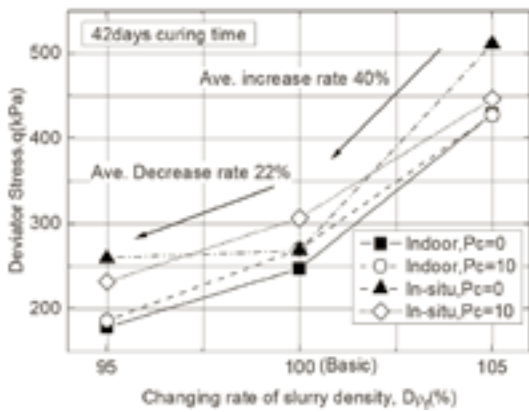


Figure 5: Relationship between the deviator stress  $q$  vs changing rate of slurry density

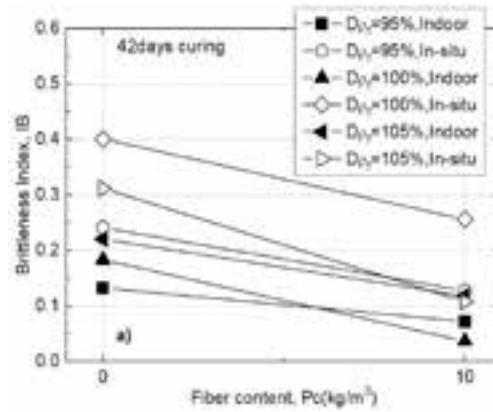


Figure 6: Fiber content vs IB

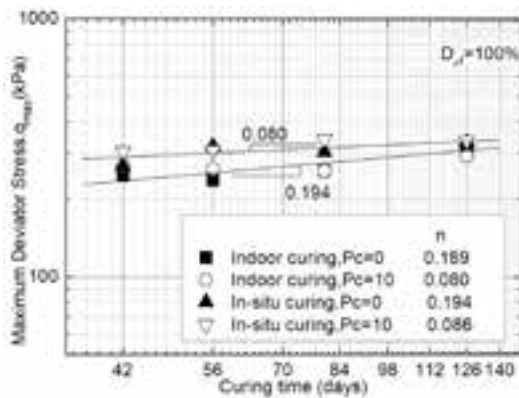


Figure 7:  $q_{max}$  vs.  $t$  relations

were poured into isolated pits excavated on the campus grounds and allowed to cure for the prescribed days (42, 56, 80, and 126 days). Figure 1 illustrates a schematic diagram of the pits. After placement, the LSS surface was covered with a polymer sheet and cured at in-situ. Using a trimmer and straight edge, the LSS blocks were excavated and formed into cylindrical specimens in the laboratory.

### 2.3. Testing method

In this study, a triaxial compression test apparatus with a pair of local deformation transducers (LDTs)<sup>4)</sup> installed on each side of the specimen was used to measure axial displacement at the small strain level and to avoid the bedding errors caused by loose layers at the top and bottom edges of the specimen and filter paper compression. A dial gauge and a proximity transducer (Gap sensor) were used to determine the axial displacement when LDTs exceeded a certain range. A series of undrained triaxial compression tests were performed at an axial strain rate of 0.054%/min, with a small unloading and reloading during the monotonic loading process. The experiments were conducted on specimens that had been cured in-situ and indoors for 42, 56, 80, and 126 days, respectively. For 15 hours, the specimens were isotropically consolidated at 98kPa confining pressure and 196 kPa back pressure before being subjected to undrained triaxial shear. Figure 2 illustrates the triaxial compression test apparatus schematically.

## 3. Results and discussion

### 3.1. Stress and strain relationships

#### 3.1.1. Effect of slurry density

Figures 3 and 4 show the relationships between deviator stress  $q$  and axial strain  $\epsilon_a$  based on locally measured axial strain by LDTs for undrained triaxial compression tests at 42 days of indoor and in-situ curing. Figure 3 shows the relationship up to  $\epsilon_a=3.5\%$ , Figure 4 shows up to 0.01% at the small strain level. It is clear from the figures that the change in slurry density influences significantly the strength of LSS both indoor and in-situ at 42 days of curing. By defining the average decreasing or increasing of maximum deviator stress as (the value that decreased or increased in maximum deviator stress) / (maximum deviator stress with basic slurry density)  $\times 100\%$ <sup>3)</sup>, the data in Figure 5 is considered that in case of larger slurry densities, the average increasing rate in indoor and in-situ curing are calculated to be about 40%, whereas the average decreasing rate with lower slurry densities are shown 30% and 14% for indoor and in-situ curing, respectively. Moreover, the maximum deviator stress,  $q_{max}$ , of in-situ LSS specimens substantially tend to be larger than that of indoor LSS ones, irrespectively of slurry density. However, in Figure 4, the gradient of the  $q$  and  $\epsilon_a$  relationship at small strains for in-situ specimens is less than that of indoor specimens, whereas in Figure 3, the  $q_{max}$  of in-situ specimens for large slurry density is large than that of indoor specimens. This indicates that when increasing slurry density at the indoor, the stiffness at small strain increased significant in comparison to the other specimens of lower slurry density that tends to only slightly increase at in-situ conditions. It caused the magnitude of viscous resistance appears to decrease with an increasing of plasticity and water content at in-situ<sup>5)</sup>. As a result, increases or decreases in slurry density have a greater influence on the stiffness of LSS at the indoor than when it is cured at in-situ.

In order to estimate the brittleness property after the peak, the brittleness index ( $I_B$ )<sup>6)</sup> was defined in this study.

$$I_B = (q_{max} / q_{res}) - 1 \quad (1)$$

Where  $q_{max}$  is the maximum deviator stress and  $q_{res}$  is the residual deviator stress. As the value of brittleness index ( $I_B$ ) decreases and approaches zero, the failure behavior becomes increasingly ductile and brittleness property is improved.

Figure 6 shows that when LSS ( $P_c=0$ ) and LSS with fiber ( $P_c=10$ ) are compared, the  $I_B$  value decreased roughly twice as fast in the specimens mixed fiber. This result can be seen as the most effective method to mix fiber into LSS to improve the brittleness mechanical property and to increase ductile performance.

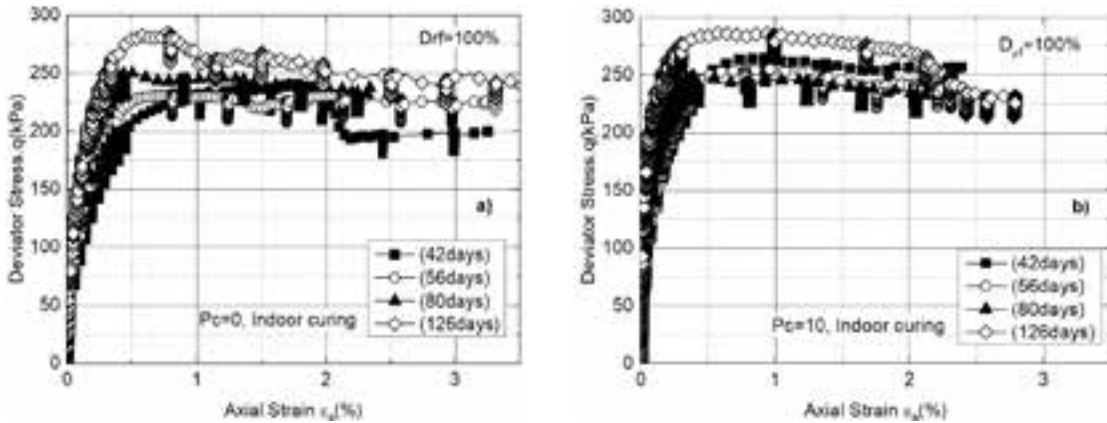


Figure 8:  $q$  vs  $\epsilon_a$  relation with  $D_{pf}=100\%$ ,  $P_c=0$

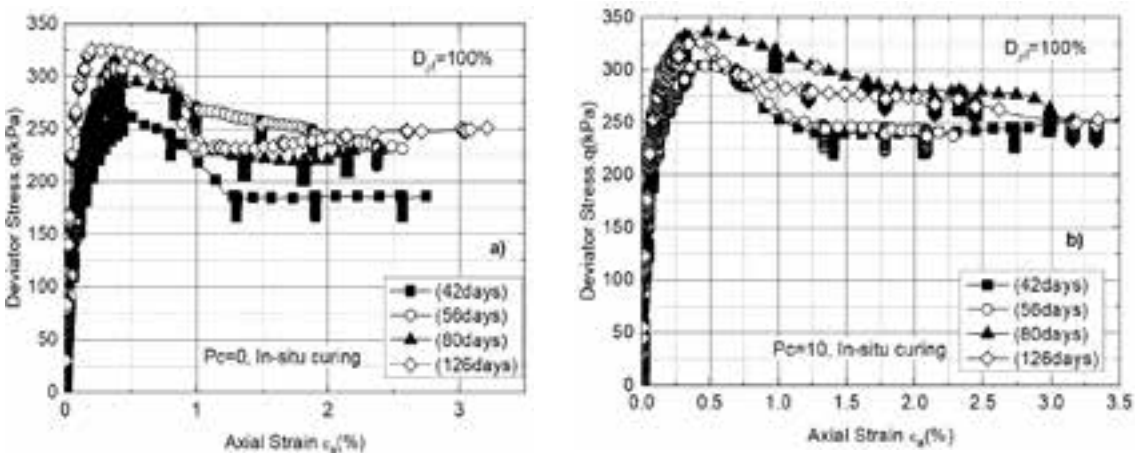


Figure 9:  $q$  vs  $\epsilon_a$  relation with  $D_{pf}=100\%$ ,  $P_c=10$

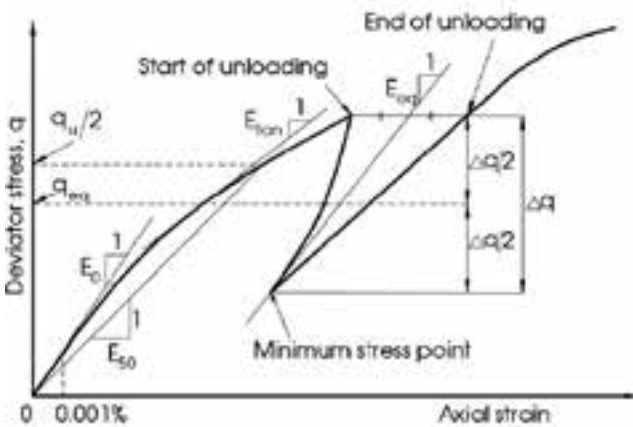


Figure 10: Definitions of  $E_0$ ,  $E_{tan}$ ,  $E_{eq}$ .

3.1.2. Effect of curing time

As shown in Figure 7 that the relationship between  $q_{max}$  and curing time  $t$  by both logarithms is linear<sup>7)</sup>  $q_{max}=a \times (t)^b$ . In both logarithm plots, the value of "n" represents the slope of the line created by a linear fit. This value becomes smaller than in cases of added fiber material ( $P_c=10$ ) and cured in-situ. It means that the effect of aging on the increasing rate of strength of LSS becomes small due the addition of fiber material and cured in-situ. Figure 8 and 9 show the relationship between  $q$  and  $\epsilon_a$  up to  $\epsilon_a=3.5\%$  based on LDTs measurement for various conditions (mixture, curing) with

a changing rate of slurry density  $D_{pf}=100\%$  at prescribed curing time. It was found that the maximum deviator stress  $q_{max}$  increased with increasing curing time in most cases.

3.2. The normalized relationships between  $E_{tan}/E_0$ ,  $E_{eq}/E_0$  and  $q/q_u$

Various Young's moduli are defined as shown in Figure 10 in this study. The initial Young's modulus  $E_0$  is defined as an initial stiffness at of  $\epsilon_a$  less than about 0.001% measured with LDTs. The  $E_{tan}$  is defined as a tangential gradient in  $q \sim \epsilon_a$  curve. This value was obtained by deviating from the fitted quadratic equation for  $q \sim \epsilon_a$  relation at a small  $\epsilon_a$  range, and it indicates the non-linearity of the deformation property in  $q \sim \epsilon_a$  curve. The value of peak-to-peak secant modulus from an unload/reload cycle is defined as the equivalent Young's modulus,  $E_{eq}$ <sup>7)</sup>, as shown in Figure 10.

Figures 11 to 14 show the normalized relationship between  $E_{tan}/E_0$  vs.  $q/q_{max}$  and  $E_{eq}/E_0$  vs.  $q/q_{max}$ , respectively, in different cases.

3.2.1. Effect of slurry density

Figures 11 a) and 11 b) showed that there was a remarkably increasing or decreasing tendency in the non-linearity of the normalized relationship between  $E_{tan}/E_0$  vs.  $q/q_{max}$  when the decreasing/increasing rate of slurry density with specimens cured at indoors was  $P_c = 0, 10$  at 42 days of curing. By contrast, the normalized tangent modulus  $E_{tan}/E_0$  exhibits a strong nonlinearity tendency when the slurry density rate is decreased and increased in in-situ specimens, as shown in Figure 11 d).

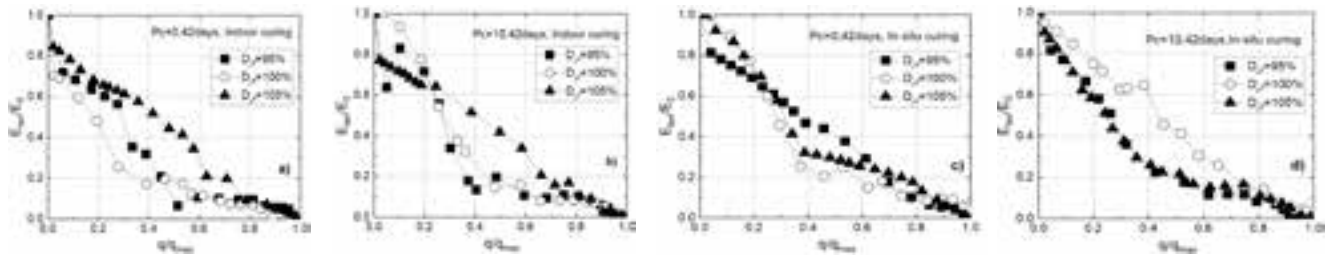


Figure 11 : Effect of slurry density on normalized relations between  $E_{tan}/E_0$  vs.  $q/q_{max}$

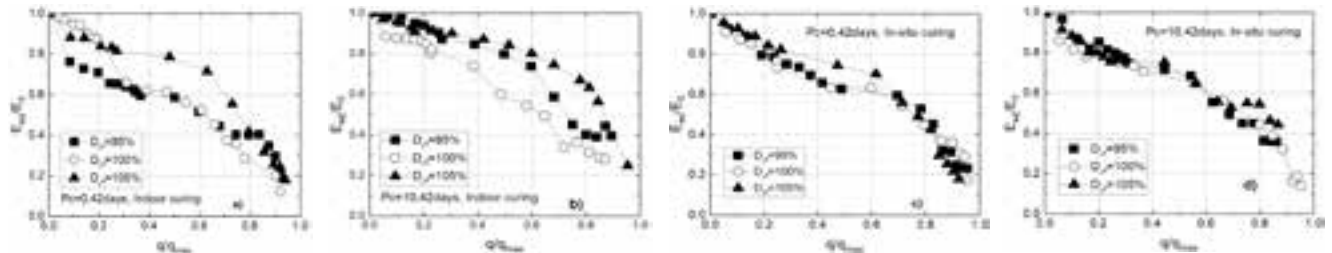


Figure 12: Effect of slurry density on normalized relations between  $E_{eq}/E_0$  vs.  $q/q_{max}$

Figure 12 shows the normalized relationship between  $E_{eq}/E_0$  and  $q/q_{max}$ . The  $E_{eq}/E_0$  value almost often increases with increasing slurry density, whereas the trend with decreasing densities is the same. However, as seen in Figure 12 d), the normalized relationship between  $E_{eq}/E_0$  and  $q/q_{max}$  seems to be generally independent of slurry density when fiber material is mixed at in-situ. As a result, the effect of changing the slurry density on the in-situ LSS added fiber material is much more non-linear in the pre-peak region, more ductile in the post-peak region, and more stable in terms of damage degree.

### 3.2.2. Effect of curing time

Figures 13 and 14 show the influence of aging time on the pre-peak non-linearity deformation property of the stress-strain relationship. There was a slightly increased normalized relation of  $E_{tan}/E_0$  with increasing curing time for LSS in both the indoor and in-situ cases, as shown in Figures 13 a) and c). The decreasing tendency of non-linearity of pre-peak deformation property is large at a long time of curing

(126 days) in most cases. However, by adding fiber material into specimens cured at in-situ, the tendency of pre-peak non-linearity behavior of the stress-strain curve seems to become rather independent of curing time in Figure 13 b) and d). Moreover, it can be seen that it is difficult to predict the influence of curing time on the non-linearity of pre-peak deformation property due to uncontrolled environmental conditions.

Figure 14 showed that the damage degree under shear stress level for indoor curing in both cases of no fiber and adding fiber seems to become more independent of curing time. Meanwhile, the  $E_{eq}/E_0$  for in-situ curing is larger than when compared with indoor cases. In particular, by mixing fiber material at in-situ, the remarkable effect of aging on the normalized relation between  $E_{eq}/E_0$  and  $q/q_{max}$  is large, as shown in Figure 14 d). In which, there was a remarkably increase in  $E_{eq}/E_0$  by curing time with normalized shear stress level due to both a decrease in the viscous deformation component during small unload/reload cycle by curing time

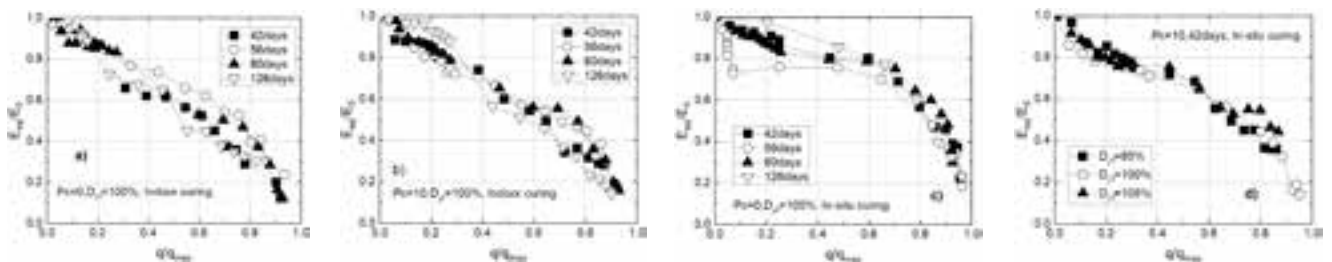


Figure 13: Effect of curing time on normalized relations between  $E_{tan}/E_0$  vs.  $q/q_{max}$

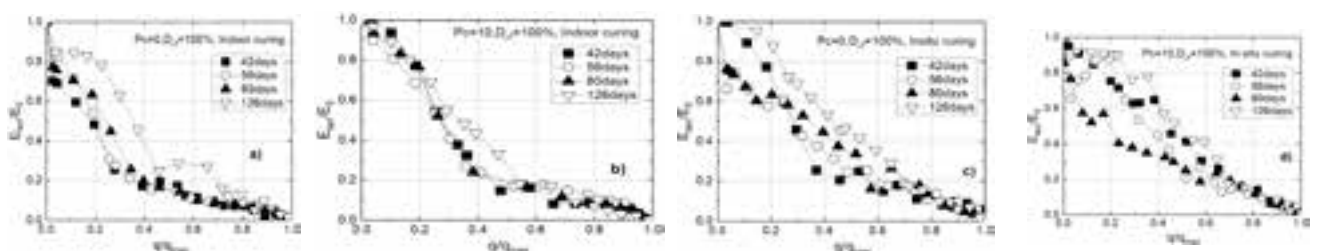


Figure 14: Effect of curing time on normalized relations between  $E_{eq}/E_0$  vs.  $q/q_{max}$

The effects of foundation depth and footing geometry are known as significant parameters, which are ignored in this

study. Therefore, it is recommended that these effects will be considered for further investigation./.

### References

1. Tran, T. T., Cao, A. T., Kim, D., & Chang, S. (2020). Seismic Vulnerability of Cabinet Facility with Tuned Mass Dampers Subjected to High-and Low-Frequency Earthquakes. *Applied Sciences*, 10(14), 4850.
2. Tran, T. T., Salman, K., Han, S. R., & Kim, D. (2020). Probabilistic Models for Uncertainty Quantification of Soil Properties on Site Response Analysis. *ASCE-ASME Journal of Risk and Uncertainty in Engineering Systems, Part A: Civil Engineering*, 6(3), 04020030.
3. M. D. Braja. *Shallow Foundation Bearing Capacity and Settlement*, 2th Edition. Taylor & Francis Group, 2009.
4. M. D. Braja. *Advanced Soil Mechanics*, 3th Edition. Taylor & Francis Group, 2008.
5. C. R. Lymon, M. I. William, Shin-Tower Wang. *Analysis and Design of Shallow and deep Foundations*. Taylor & Francis Group, 2006.
6. H. A. Taiebat, J. P. Carter. *Bearing capacity of strip and circular foundation on undrained subjected to eccentric loads*. *Geotechnique* 52(1) (2002) 61 – 64.
7. S. Gupta, A. Mital. Numerical analysis of bearing capacity of rectangular footing. *Journal of Physics: Conference Series* 1240(1) (2019) 012039.
8. B. Móczár, J. Szendefy. Calculation of presumed bearing capacity of shallow foundation according to the principles of Eurocode 7. *Periodica Polytechnica civil engineering* 61(3) (2017) 505 – 515.
9. C. Atala, C. R. Patra, B. M. Das, N. Sivakugan. Bearing capacity of shallow foundation under eccentrically inclined load. *Proceedings of the 18th international coference on Soil mechanics and Geotechnical engineering* (2013) 3439-3442.
10. P. Vo, D. D. Nguyen. Assessment of load bearing capacity of liquefied sandy ground under raft foundation. *Journal of Science Ho Chi Minh City Open University* 51(6) (2016) 68-79.
11. D. L. Nguyen, S. Ohtsuka, K. Kaneda. Utimate bearing capacity of footing on sandy soil against combined load of vertical, horizontal and moment loads. *Int. J. of Geomate* 10(1) (2016) 1649-1655.

## The effect of aging and slurry density on triaxial shear properties...

(tiếp theo trang 27)

with shear stress, and an increase in the elastic component of strain by aging in in-situ specimens. This property is similar to that of cement-treated gravelly soil<sup>5</sup>).

### 4. Conclusions

Base on the results of a series of undrained triaxial compression tests on LSS mixed with fibered materials and LSS, the following conclusions were obtained.

1) The slurry density had a considerable effect on the strength of LSS. When slurry density is increased, the strength increases by about 40% for both indoor and in-situ curing, whereas reducing slurry density decreases the strength by about 30% and 14% for indoor and in-situ curing, respectively.

2) The influence of shear stress level on the degree of damage appears to be independent of slurry density in case of in-situ curing. This result has practical implications for the application of LSS to increase seismic resistance.

3) By both logarithms, the relationship between  $q_{max}$  and the curing time  $t$  of LSS is linear. The effect of curing time on the increasing rate of strength is small in compared to indoor specimens of LSS.

4) By adding fiber into in-situ cured LSS, the effect of curing time on the degree of damage is found to be largely due to a decrease in viscous deformation and an increase in the elastic component of strain.

### 5. Acknowledgement

The authors express deep gratitude to Mr. Moteki, Mr. Onodera (formerly, graduate and undergraduate student), and Ms. Watanabe, Mr. Okada, and Ms. Xi (undergraduate student of Muroran Institute of Technology) for sample preparation, experiments and data analysis. This work was supported by JSPS KAKENHI Grant Number JP19K04590 (Grant-in-Aid for Scientific Research(C))./.

### References

1. G. Kuno, eds. *Liquefied stabilized soil method Recycling technology of construction-generated soil and mud*. Gihodo publication, 1997 (in Japanese).
2. K. Ito, Y. Kohata, and Y. Koyama. Influence of additive amount of cement solidification on agent on mechanical characteristics of Liquefied Stabilized Soil mixed with fibered material. *Japanese Geotechnical Society Hokkaido Branch Technical Report Papers*, Vol.51, 131-136, 2011 (in Japanese).
3. Y. Cui and Y. Kohata. Influence of cement solidification agent and slurry density on mechanical property of liquefied stabilized soil. *International Journal of GEOMATE*, Vol.19, Issue 73, 177-184, 2020.
4. S. Goto, F. Tatsuoka, S. Shibuya, Y-S. Kim, and T. Sato. A simple gauge for local small strain measurements in the laboratory. *Soils and Foundations*, Vol. 31, No. 1. 169-180, 1991.
5. F. Tatsuoka, and L. Kongsukprasert. Small strain stiffness and non-linear stress-strain behavior of cement-mixed gravelly soil. *Soils and foundations*, Vol.47, No.2, 375-394, 2007.
6. NC. Consoli, JP. Montardo, PDM. Prietto, and GS. Pasa. Engineering behavior of a sand reinforced with plastic waste. *J Geotech and Geo Environ Eng.*, Vol. 128, Issue6, 462-472, 2002.
7. F. Tatsuoka and Y. Kohata. Stiffness of hard soils and soft rock in engineering applications. *Pre-failure deformation of Geomaterial*, Balkema, Vol.2, 1030-1035, 1995.